Macromolecules

Article

pubs.acs.org/Macromolecules

Patternable Conjugated Polymers with Latent Hydrogen-Bonding on the Main Chain

Kun Yang, Tianda He, Xiaoyi Chen, Stephen Z. D. Cheng, and Yu Zhu*

Department of Polymer Science, College of Polymer Science and Polymer Engineering, The University of Akron, 170 University Circle, Akron, Ohio 44325-3909, United States

Supporting Information

ABSTRACT: Conjugated polymers with latent hydrogen-bonding on the main chain were synthesized using Suzuki coupling reaction. The resulting polymers with latent hydrogen-bonding can be converted to the actual hydrogen-bonded polymers by thermal annealing or UV irradiation. As the hydrogen-bonding sites are fused with π-conjugated units on the polymer backbone, the intermolecular interactions between the polymer chains will be strongly enhanced when the hydrogen-bonds are formed. By removing the protection group and forming hydrogen-bonding, the polymers exhibited a bathochromic shift over those with latent hydrogen-bonding, indicating a hydrogen-bonding-mediated enhancement of $\pi-\pi$ stacking. In addition, the fused hydrogen-bond sites and π-conjugated units led to closely packed polymer chains, resulting in insoluble pigment-like polymers. This drastic solubility change from polymers with latent hydrogen-bonding to hydrogen-bonded polymers can be used to pattern conjugated polymers directly. The photolithography of the conjugated polymer with latent hydrogen-bonding was demonstrated, and the patterned electrochromic devices were fabricated and tested.

INTRODUCTION

The organic electronics developed rapidly in the past two decades[1,2] due to their advantages in fabricating lightweight, flexible, and low-cost electronic components. The organic electronic devices such as organic light-emitting devices (OLEDs), organic field-effect transistors (OFETs), and organic photovoltaics (OPVs) have been demonstrated,[3,4] and some have been commercialized.[5,6] Among all the materials for organic electronics, conjugated polymers comprise a class of materials that have the potential to provide low-cost, large-area, and flexible electronic devices. Although the conjugated polymers have been demonstrated in prototype devices that they are in principle suitable for many electronic applications, the implementation of those electronic devices often requires the patterning of conjugated polymers into microregimes to provide various functions.[7−9] For instance, the micropatterning of conjugated polymer is required prerequisite to fabricate the polymer-based OFETs circuit,[10] OLDEs,[11] and electrochromic displays.[12,13] For this purpose, many patterning techniques such as inkjet printing,[14−16] microcontact printing,[17,18] and nanoimprinting[14,19] have been developed to pattern organic electronic materials. Among those techniques, conventional photolithography is of great interest due to the mature industrial scale photolithography instruments from Si-based electronics. Therefore, the conjugated polymers with patterning function that can adopt conventional photolithography technology are highly desired. Photopatterning of conjugated polymer has been explored by some researchers.[20−27] Most works were relied on the approach to directly adjust the solubilities of conjugated polymers through photochemistry, although research of photolithographically patterning conjugated polymers with additional parylene[21] protect layer or special fluorinated photoresist[22] have been reported as well. The common technique to adjust solubility during the photolithography process is to introduce cross-linkable side chains on the conjugated polymers. The radical polymerization of acrylates,[25,26,28−31] oxetane ring-open polymerization,[11,23,24,27,32−37] and [2 + 2] cycloaddition between cinnamates and chalcones[38−40] were used in cross-linkable conjugated polymers. With the help of cross-link-based solubility control methods, the multilayer devices have been demonstrated.[11,35] The solubility of the polymer can be adjusted by using labile groups as well.[41] However, the removal of the labile group is usually very tedious.

Here we demonstrated a facile strategy to pattern the conjugated polymers by latent hydrogen-bonding. In this new strategy, the conjugated units with fused hydrogen-bonding sites are designed or adopted. The removable group (*N*-*tert*-butoxycarbonyl, *t*-Boc) was used to block hydrogen-boning sites, and then the soluble polymers with latent hydrogen-bonding can be synthesized. After the removal of *t*-Boc group by thermal or UV (ultraviolet) irradiation, the actual hydrogen-bonded polymer can be formed. Because the hydrogen-bonding sites are fused with conjugated unit, the resulting rigid hydrogen-bonded polymers show very low solubility in organic solvents that are used to process polymers with latent hydrogen-bonding. A similar solubility change intrigued by hydrogen-bonding was

Received: September 22, 2014
Revised: November 24, 2014

   dx.doi.org/10.1021/ma501960t | *Macromolecules* XXXX, XXX, XXX−XXX

Scheme 1. Synthesis Scheme of Conjugated Polymers with Latent Hydrogen-Bonding[a]

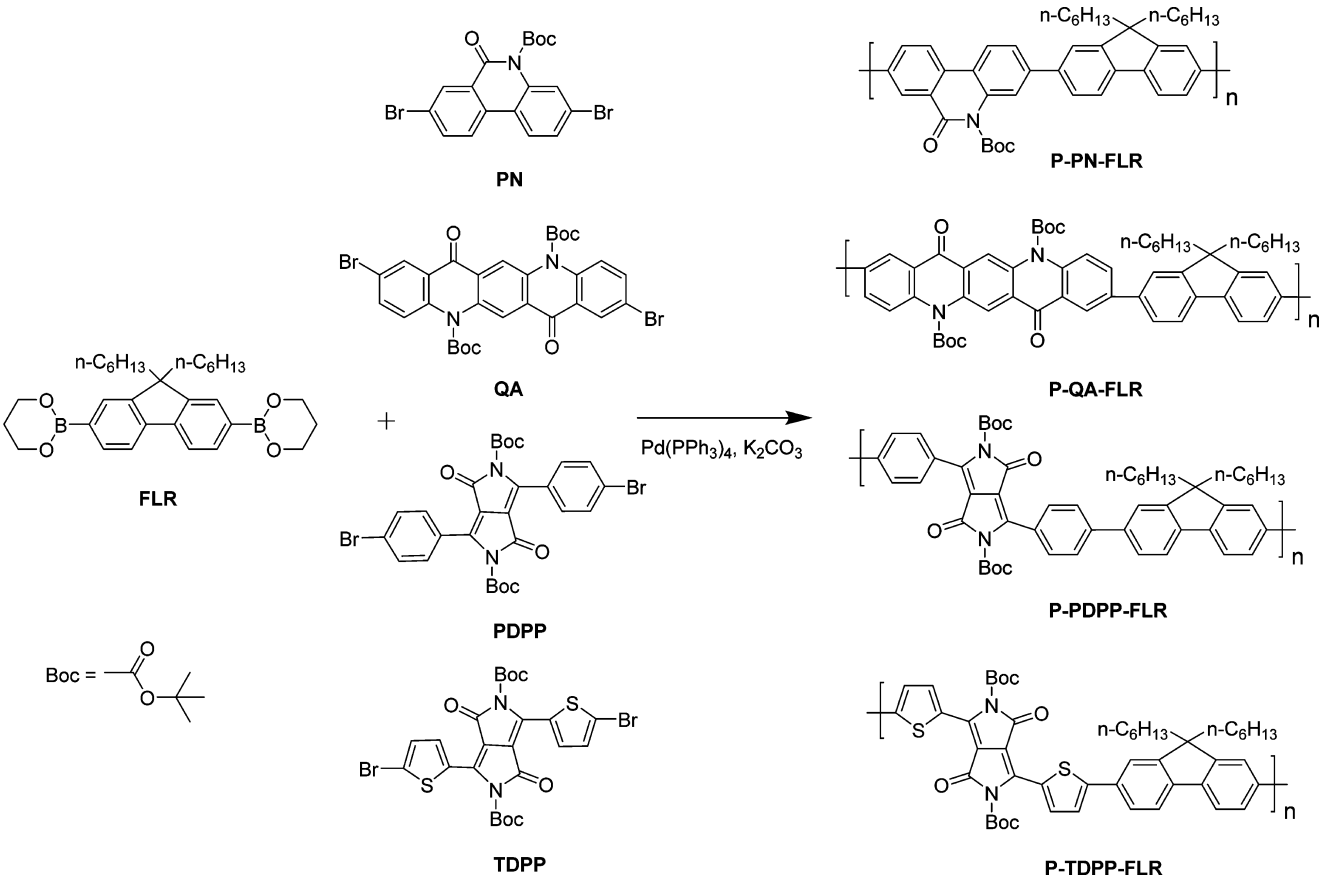

[a]Four polymers are demonstrated in this work with *t*-Boc groups on the phenanthridinone (PN), quinacridone (QA), and diketopyrrolopyrrole units (PDPP ad TDPP). The Suzuki−Miyaura polymerization is used to synthesize the polymers.

reported in small molecular pigments.[42,43] Compared with cross-link based method,[11] this new strategy can obtain polymers with high percentage of conjugated content. Compared with the labile group based patterning technique,[41] the new method in this work is more efficient and can be carried out under milder conditions. We have demonstrated this technique can be used to pattern electrochromic devices.

RESULTS AND DISCUSSION

Polymer Synthesis. The synthetic scheme of the conjugated polymers with removable side chain is illustrated in Scheme 1. Four new polymers containing the *t*-Boc group were synthesized in this work. All polymers contain one fluorene unit (FLR) and one conjugated unit with latent hydrogen-bonding group. 3,8-Dibromophenanthridinone (PN) was synthesized from 2,7-dibromofluorenone by the Schmidt reaction,[44] while dibromoquinacridone (QA),[45] 1,4-diketo-3,6-bis(4-bromophenyl)-pyrrolo[3,4-*c*]pyrrole (PDPP),[46] and 1,4-diketo-3,6-bis(4-bromothienyl)pyrrolo[3,4-*c*]pyrrole (TDPP)[47] were synthesized based on the modified procedure in previous reports. In a general procedure to protect the lactam group with the *t*-Boc group, the monomers were treated with di-*tert*-butyl dicarbonate in the existence of 4-(dimethylamino)pyridine (DMAP). The resulting *t*-Boc-substituted monomers exhibited good solubility and were used in the polymerization. The polymers were synthesized by Suzuki−Miyaura polymerization.[48] The resulting polymers were soluble in common organic solvents such as chloroform, toluene, and tetrahydrofuran. A detailed synthesis procedure and characterization of the polymers are described in Experimental Section and Supporting Information. The polymers are used for the following study directly.

Immobilization. In order to study the immobilization property of polymer films, thermal annealing experiments were conducted to remove the *t*-Boc group from polymers. The casted polymer films on glass substrates were annealed in an isothermal chamber at 180 °C for 5 min. Compared with the similar strategy used in the literature,[41] the immobilization condition in this work is much milder. The UV/vis spectra of the polymer films before and after thermal annealing are shown in Figure 1. For comparison, the UV/vis spectra of the monomer and polymer solution are presented in Figure 1 as well. The absorbance onset wavelength of the monomers, polymer solutions, and polymer solid films are listed Table S1. As shown in Figure 1 and Table S1, a bathochromic shift is observed for all polymers films after thermal annealing (based on the onset absorption wavelength of polymer solid films). The bathochromic shifts of polymers P-QA-FLR (65 nm) and P-PDPP-FLR (35 nm) are very large. This can be explained as the enhancement of $\pi-\pi$ stacking by removing bulky group and forming hydrogen-bonding (Supporting Information, Figure S13). Similar hydrogen-bonding-mediated enhancement of $\pi-\pi$ stacking has been observed on the quinacridone[43] and diketopyrrolopyrrole pigments.[42] The annealed polymers also became insoluble in the casting solvent (THF) and many other solvents such as water, chloroform, and hexane. The solubility of the annealed polymer films was quantitatively examined (Supporting Information, Figure S2).

dx.doi.org/10.1021/ma501960t | *Macromolecules* XXXX, XXX, XXX−XXX

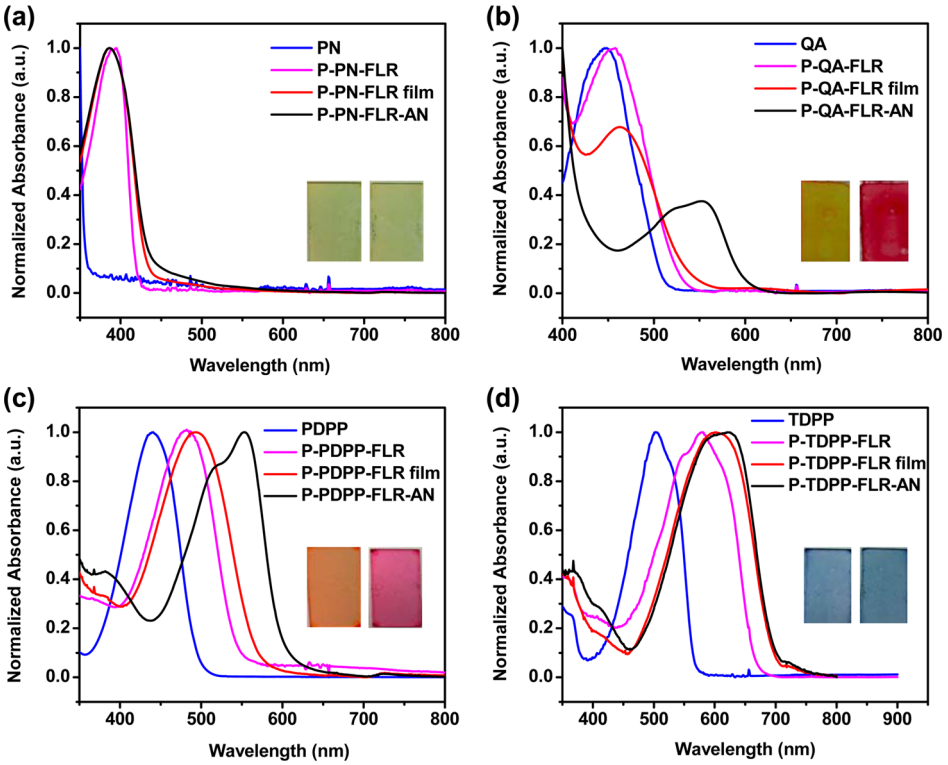

Figure 1. Normalized UV/vis spectra of monomers and polymers: (a) P-PN-FLR; (b) P-QA-FLR; (c) P-PDPP-FLR; (d) P-TDPP-FLR. Blue curve: monomers in THF solution; magenta curve: polymers in THF solution; red curve: polymer films on glass; black curve: polymer films on glass after thermal annealing. Insets show the optical images of polymer films before (left photo in all cases) and after (right photo in all cases) thermal annealing.

The results indicated that the intensity of the absorbance remained between 92% and 97% after solvent washing. Those results indicated that an actual hydrogen-bonded polymer (Scheme 2) was formed after thermal annealing.

Scheme 2. Scheme of an Actual Hydrogen-Bonded Polymer

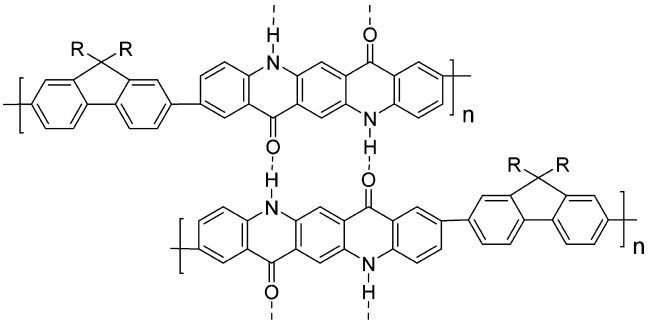

Fourier transform infrared spectroscopy (FT-IR) was used to investigate the chemical structure changes upon annealing. As shown in Figure 2, the absorption peak for the carbonyl group in *t*-Boc group (from 1680 to 1810 cm^{-1}, red frame shadowed area in Figure 2) disappeared after annealing, indicating a full removal of *t*-Boc group in the solid polymer film. Furthermore, a new peak appeared between 3170 and 3250 cm^{-1} (green frame shadowed area in Figure 2), resulting from the N−H bond.[49] Other peaks on the FTIR spectra remained similar in all four polymers, suggesting that the only change during the annealing was the deprotection of *t*-Boc group. Thermogravimetric analysis (TGA) further confirmed these results (Supporting Information, Figure S3), The weight losses at 180 °C matched the weight percentage of the *t*-Boc group in the polymer very well. Therefore, the drastic change of the solubilities before and after annealing can be explained by the removal of the solubility-promoting side chain as well as the formation of hydrogen bonds between polymer molecules.

Electrochemical Properties. The electrochemical properties of the polymers with latent hydrogen-bonding and polymers with actual hydrogen-bonding are investigated. The cyclic voltammetry (CV) results of the polymer films before and after thermal annealing are shown in Figure 3. The oxidation and reduction onset potentials, highest occupied molecular orbital (HOMO) and lowest unoccupied molecular orbital (LUMO) levels, electrochemical band gaps, and the optical band gaps of both nonannealed and annealed polymer films are summarized in Table 1. All nonannealed and annealed polymers exhibited oxidation peaks between 0.63 and 1.12 V (vs Fc/Fc^{+}) and reduction processes between −2.07 and −1.01 V (vs Fc/Fc^{+}). Table 1 also indicates that the oxidation onset potentials of annealed polymer film are lower than those of nonannealed polymers. In addition, the reversibility of the oxidation process for P-PDPP-FLR is improved after thermal annealing, as shown in Figure 3e,f. This can be explained by the fact that the annealed polymers have very low solubility in electrolyte solution. During the CV of nonannealed polymer films, a typical phenomenon was that the polymers became soluble at oxidative states due to the formation of charged polymer molecules. As a result, the polymer could not stay on the ITO electrode and the reversibility of the CV became poor. However, for the annealed polymers, the dissolving of charged polymer film did not occur; thus, the reversibility of the polymer was enhanced.

Based on the onset potentials, the HOMO/LUMO levels and electrochemical band gap of polymers were calculated. These results matched the optical band gap very well. The band gaps of

dx.doi.org/10.1021/ma501960t | *Macromolecules* XXXX, XXX, XXX−XXX

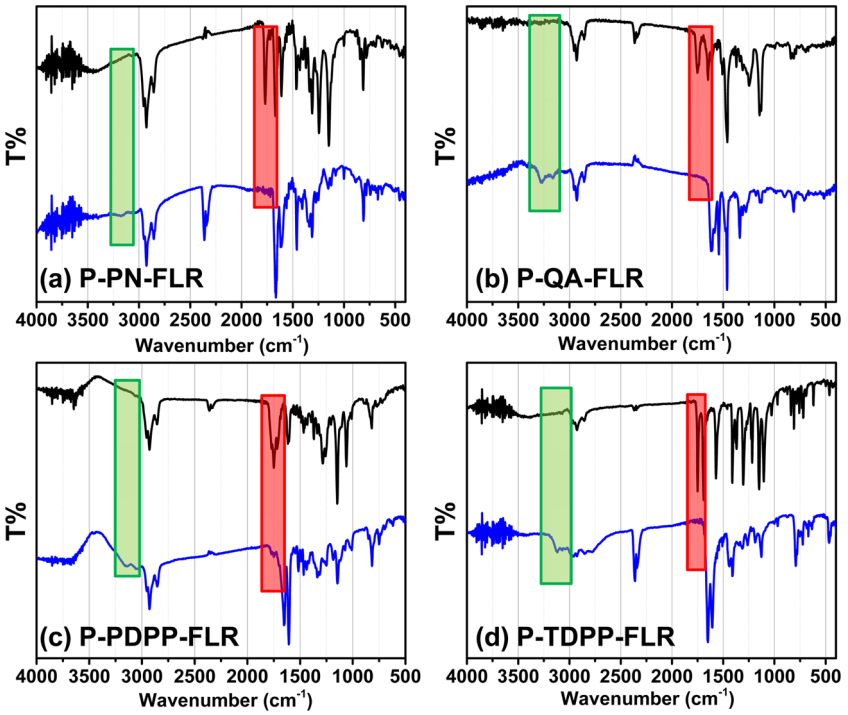

Figure 2. FT-IR spectra of polymer films on KBr crystal plate before (black curve) and after (blue curve) thermal annealing: (a) P-PN-FLR; (b) P-QA-FLR; (c) P-PDPP-FLR; (d) P-TDPP-FLR. The red frames indicate the region where the absorption peaks of *t*-Boc group appears. The green frames show that the new absorption peaks related to the hydrogen-bonding.

P-PN-FLR and P-TDPP-FLR only change slightly after thermal annealing process, while P-QA-FLR and P-PDPP-FLR showed much narrower band gap after annealing. The results agreed well with the UV/vis spectra, and the decrease of band gap can be explained as the hydrogen-bonding mediated $\pi-\pi$ stacking enhancement.[42]

Electrochromism is a typical phenomenon of semiconductive polymers. Thus, the spectroelectrochemical analysis was conducted for the polymers before and after thermal annealing. The typical spectroelectrochemical results are shown in Figure 4 a,b (for polymer P-PN-FLR). In the neutral state, polymer P-PN-FLR film exhibited an absorption peak around 387 nm that arose from the $\pi-\pi^*$ electronic transition of polymer molecules. When the applied potential was increased, the absorption peak at 387 nm began to diminish and a new broad peak centered at 515 nm appeared. This was due to the absorption from the polarons formed in the oxidized state.[50] The polymer P-PN-FLR therefore showed a sharp color change from nearly transparent neutral state to red oxidized state (Supporting Information, Video S1). The isosbestic point observed at about 420 nm also indicated that the oxidation of the polymer was accomplished with a single-step electronic transition of the polymer backbone.[51] Spectroelectrochemistry of the annealed polymer P-PN-FLR film was similar to that of the nonannealed film; nonetheless, the switching voltage is slightly lower, and the absorption maxima for the neutral and oxidative states are 386 and 523 nm, respectively. For other three groups of nonannealed and annealed polymer films, similar spectroelectrochemical processes were observed (Supporting Information, Figures S4–S6). However, their color change profiles were different. It is worth to notify that the color switching profile for P-PN-FLR is very interesting for practical electrochromic devices. It has transparent neutral state and red oxidized state. In most electrochromic polymer reported previously,[52] the transparent state is achieved in the oxidized state where the polaron is formed and the absorption spectrum is shifted to the IR range. If the electrochromic devices need to be kept at bleached state more frequently than the colored state, the material showing anodically coloring is preferred: it decreases the energy consumption of the device, and more importantly, it extends the lifetime of the device because the polaron state is usually more sensitive to the environment than the neutral state. The electrochromic switching response of P-PN-FLR films was examined. In this experiment, the absorbance changes at the maximum absorption wavelength (515 nm for nonannealed film and 523 nm for annealed film) were recorded when the voltage applied on the film was switched from −0.23 and 1.17 V (vs Fc/Fc$^+$). As shown in Figure 4c, the switch times (at 50% absorbance change) for nonannealed polymer P-PN-FLR film and annealed polymer P-PN-FLR film were 1.2 and 0.6 s, respectively. The results indicated that a quicker response was observed after the removal of the *t*-Boc group from the polymer, possibly due to a higher concentration of π-conjugated units in the whole polymer structure for annealed polymer film. As the only difference is the *t*-Boc group for the nonannealed P-PN-FLR and annealed P-PN-FLR, this result also suggested that the polaron might be formed on the phenanthridinone unit of the P-PN-FLR. The cyclability of the polymer P-PN-FLR was then investigated. A continuous voltage switching between −0.23 and 1.17 V (vs Fc/Fc$^+$) was applied on the polymer films while the optical absorption at 520 nm was measured *in situ*. As shown in Figure 4d, both annealed polymer and nonannealed polymer films showed good stability after 100 cycles.

Photopatterning. The *t*-Boc group can be removed by not only thermal annealing but also the acid treatment.[53,54] Therefore, the *t*-Boc group-functionalized conjugated polymers in this work are in principle patternable with the conventional photolithography technique. The photolithography method used in this work is illustrated in Scheme 3. The photoacid

dx.doi.org/10.1021/ma501960t | *Macromolecules* XXXX, XXX, XXX–XXX

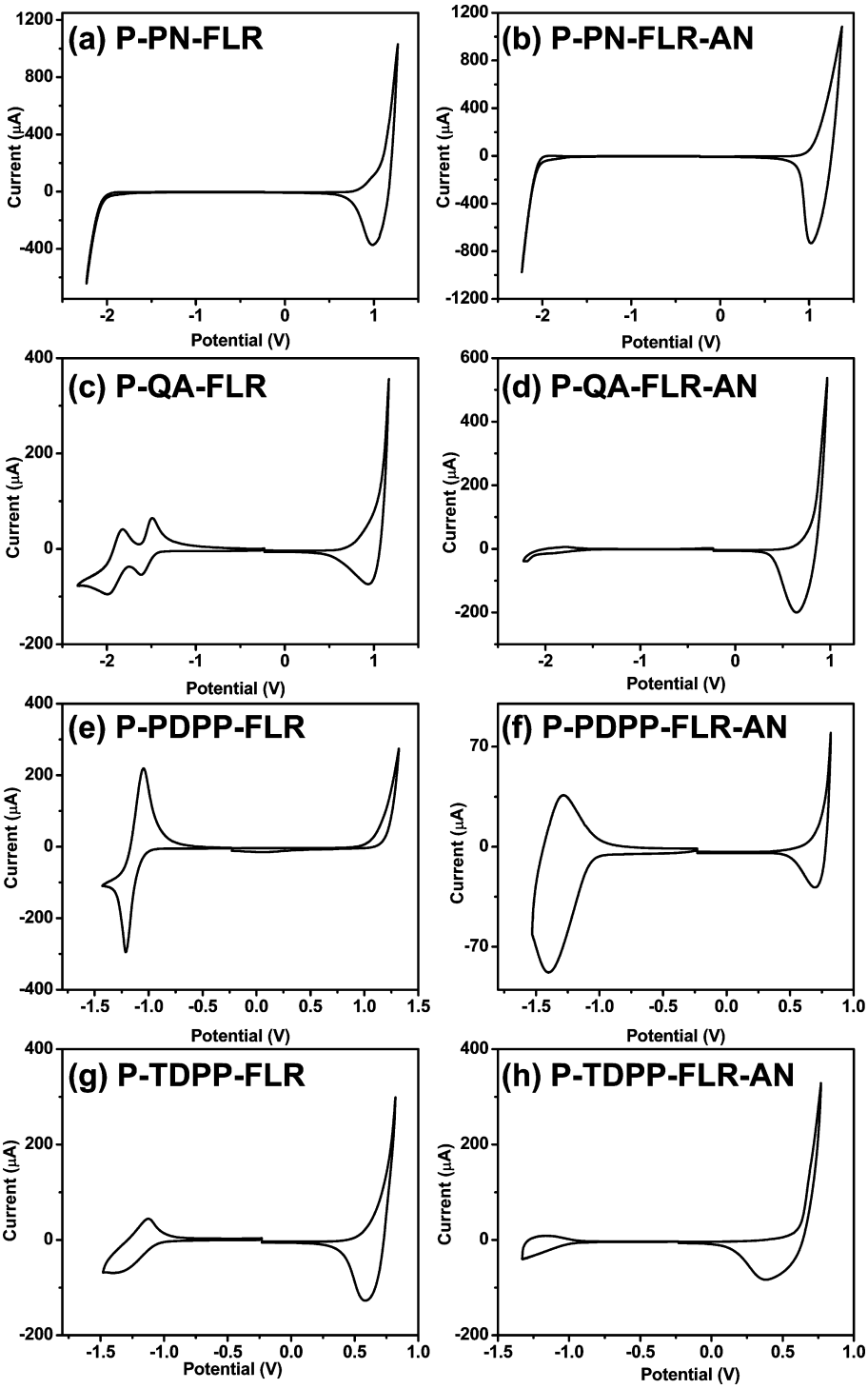

Figure 3. Cyclic voltammograms of polymer films. (a, b) P-PN-FLR and P-PN-FLR-AN. (c, d) P-QA-FLR and P-QA-FLR-AN. (e, f) P-PDPP-FLR and P-PDPP-FLR-AN. (g, h) P-TDPP-FLR and P-TDPP-FLR-AN. AN indicates the annealed polymer films. Electrolyte: 0.1 M $TBAPF_6/CH_3CN$. Potential calculated versus Fc/Fc^+. Scan rate: 50 mV/s; T = 25 °C.

generator (4-phenylthiophenyl)diphenylsulfonium triflate was used to remove the *t*-Boc group from the polymer backbone. In order to minimize the contamination of conjugated polymers by (4-phenylthiophenyl)diphenylsulfonium triflate, the triflate solution (in methanol) was overcoated on the conjugated polymer film by spin-coating, which can be washed away after patterning (see Supporting Information photopatterning procedures for details) After UV irradiation, similar solubility change as thermal annealing treatment was observed. The patterns on photomask can be transferred on the polymer film by rinsing the samples with suitable solvent, similar to a negative-tone photoresist. The patterning was carried out under ambient condition and the resulting patterned polymer film still exhibited excellent electrochromic property (Figure 5 and Supporting Information Video S2). As shown in Figures 5a and 5b, the patterned P-PN-FLR films was transparent at neutral state and showed red "UA" letters at the oxidized state. The UV/vis spectra, FTIR spectra, and electrochemical and spectroelec-

dx.doi.org/10.1021/ma501960t | *Macromolecules* XXXX, XXX, XXX–XXX

Table 1. Optical and Electrochemical Properties of Nonannealed and Annealed Polymers[a]

polymers	λ_{film} [nm]	$E_{g,opt}$ [eV]	V_{ox} [V]	E_{HOMO} [eV]	V_{red} [V]	E_{LUMO} [eV]	$E_{g,ec}$ [eV]
P-PN-FLR	431	2.88	1.08	−5.88	−2.07	−2.73	3.15
P-PN-FLR-AN	435	2.85	1.07	−5.87	−2.07	−2.73	3.14
P-QA-FLR	536	2.31	1.02	−5.82	−1.44	−3.36	2.46
P-QA-FLR-AN	601	2.06	0.82	−5.62	−1.49	−3.31	2.31
P-PDPP-FLR	569	2.18	1.12	−5.92	−1.09	−3.71	2.21
P-PDPP-FLR-AN	604	2.05	0.73	−5.53	−1.06	−3.74	1.83
P-TDPP-FLR	693	1.79	0.68	−5.48	−1.04	−3.76	1.72
P-TDPP-FLR-AN	700	1.77	0.63	−5.43	−1.01	−3.79	1.64

[a] λ_{film}: UV/vis onset absorption wavelength; $E_{g,opt}$: optical bandgap; V_{ox}: oxidation onset potential; E_{HOMO}: HOMO level; V_{red}: reduction onset potential; E_{LUMO}: LUMO level; $E_{g,ec}$: electrochemical bandgap. HOMO/LUMO are calculated based on the equations $-E_{HOMO} = (E_{ox} + 4.8)$ [eV], $-E_{LUMO} = (E_{red} + 4.8)$ [eV], and $E_{g,ec} = E_{LUMO} - E_{HOMO}$. Optical band gap is obtained from absorption onset wavelength (λ_{film}) by using the equation $E_{g,opt} = 1240/\lambda_{film}$ [eV] (nonannealed films: P-X-FLR; annealed films: P-X-FLR-AN, X = PN, QA, PDPP, or TDPP).

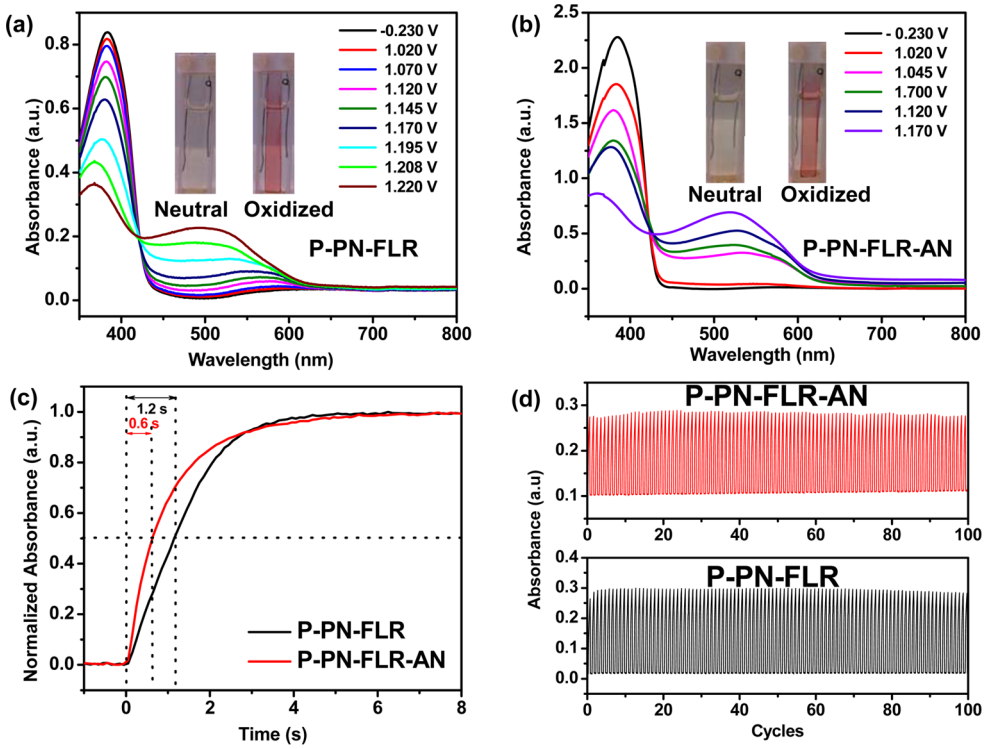

Figure 4. (a, b) Spectroelectrochemical analysis of P-PN-FLR film on an ITO anode before (a) and after (b) thermal annealing. (c) Absorbance (at maximum absorption wavelength) of P-PN-FLR film vs response time when the applied voltage is switched from −0.23 to 1.17 V. The switch times at 50% absorbance are 1.2 and 0.6 s for nonannealed film and annealed film, respectively. (d) Plots of absorbance vs number of cycles for repeated chronocoulometry cycling of P-PN-FLR film (black) and annealed P-PN-FLR film (red). Electrolyte: 0.1 M $TBAPF_6$ in CH_3CN. All the potentials were corrected to Fc/Fc^+ standard. The insets in (a) and (b) are the optical images of polymer P-PN-FLR films under neutral and oxidized states.

trochemical characterization of the photopatterned polymer P-PN-FLR are summarized in Figure S7 and Table S2. The photopatterned polymer shows similar properties as the thermal annealed samples.

As this patterning process is fully compatible with conventional photolithography, it can be used to pattern conjugated polymers with much higher resolution. In Figure 5c,d and Figure S8, the fine patterns with different length features from 25 to 125 μm have been demonstrated. Figure 5c is the SEM image of polymer patterned with a TEM grid shadow mask. Figure 5d shows the patterned polymer squares (100 × 100 μm) on the silicon wafer with the distance of 25 μm between the polymer blocks. It is worth noting that the resolution of the pattern here is limited by the stencil masks that are commercial available. It is theoretically possible to get even higher resolution with this technique if a more delicate mask is applied. This can be very useful since multilayered structures are commonly used in many organic electronic devices such as OPVs, OFETs, and OLEDs. The fabrication of pixel-based electrochromic displays[55] is also possible with the polymers developed in this work.

CONCLUSION

In this report, a class of novel conjugated polymers with latent hydrogen-bonding on the main chain have been synthesized and characterized. The switching from the latent hydrogen-bonding state to actual hydrogen-bonded state can lead to dramatic solubility change. This phenomenon allows the direct patterning of conjugated polymers as a negative-tone photoresist with conventional photolithography technique. Some hydrogen-bonded polymers also exhibited strong interchain interaction, resulting in large bathochromic shifts in the UV/vis spectra. The

dx.doi.org/10.1021/ma501960t | Macromolecules XXXX, XXX, XXX−XXX

Scheme 3. Scheme of the Photolithography Process and Electrochromic Demonstration of the Polymers

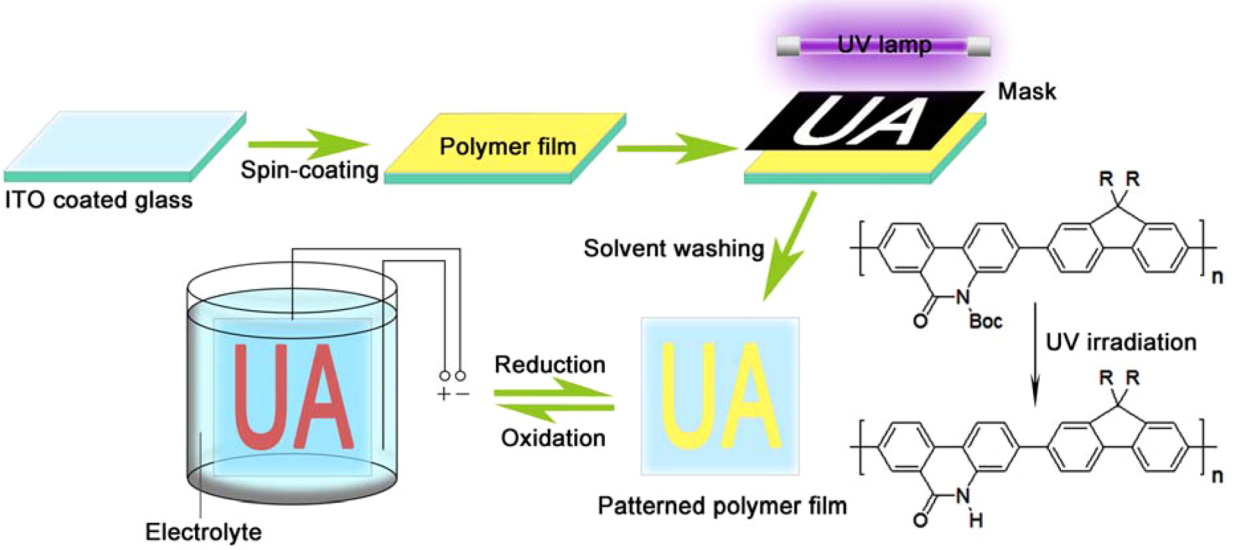

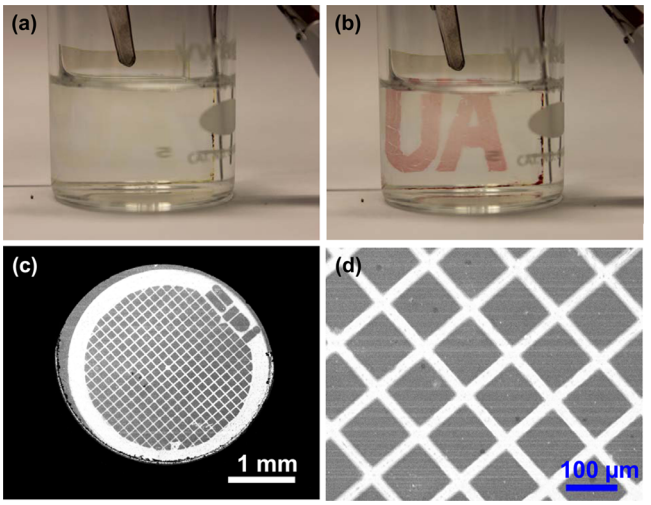

Figure 5. Images of the photolithograhy patterned polymer films. (a) Patterned polymer P-PN-FLR on ITO glass at neutral state. (b) Patterned polymer P-PN-FLR on ITO glass at oxidized state. (c) SEM image of patterned polymer P-PN-FLR film (through a TEM grid shadow mask) on silicon wafer. (d) High-resolution SEM image of patterned P-PN-FLR film on silicon wafer (the dark regions are covered with polymer).

electrochromic properties of the polymers have been investigated. The polymer P-PN-FLR showed excellent anodically coloring red, which is different from widely reported cathodically coloring red conjugated polymers. The photolithography patterned electrochromic device has been demonstrated. This study provides a new strategy for patternable conjugated polymers.

EXPERIMENTAL SECTION

General Polymer Synthesis. 200 mg of (0.44 mmol) *tert*-butyl 3,8-dibromo-6-oxophenanthridine-5(6*H*)-carboxylate (PN), 228.98 mg of 9,9-dihexylfluorene-2,7-diboronic acid bis(1,3-propanediol) ester (0.44 mmol, 1.0 equiv, Sigma-Aldrich, 97%), and 15.37 mg of $Pd(PPh_3)_4$ (3% equiv) were charged into a flask with 1 mL of *p*-dioxane and 2 mL of toluene. The mixture was degassed for 3 min using ultrasonication and then heated to 80 °C under N_2 protection. A degassed K_2CO_3/water (153 mg of K_2CO_3, 2.5 equiv in 1 mL of water) solution was added in one portion, and the temperature was raised to 105 °C for 2.5 h. Then the reaction mixture was cooled, and 40 mL of toluene was added. After washed with brine (30 mL × 2) and water (30 mL), the organic phase was dried over Na_2SO_4 and evaporated. The solid was dissolved in a minimum amount of CH_2Cl_2 and precipitated in a small amount of methanol. The polymer was collected and dried under vacuum. 150 mg of product (P-PN-FLR) was obtained with yellow color (54%). M_w: 30 000, PDI: 2.0. ^{1}H NMR (300 MHz, $CDCl_3$): δ 8.92 (1H), 8.41 (1H), 8.19 (1H), 7.9−7.6 (8H), 7.50 (1H), 2.12 (4H), 1.83 (9H), 1.2−0.7 (22H).

Synthesis and characterization of the polymers P-QA-FLR, P-PDPP-FLR, and P-TDPP-FLR are similar and shown in the Supporting Information.

Electrochemistry. Cyclic voltammetry (CV) analysis of the polymer films were carried out in a three-electrode cell with *tetra-n*-butylammonium hexafluorophosphate ($TBAPF_6$, 0.1 M in acetonitrile) as the supporting electrolyte, an indium-doped tin oxide (ITO) glass casted with polymer films as the work electrode, and two platinum wires as the counter electrode and reference electrode. The scan rate is 50 mV/s, and all the potentials were corrected to the ferrocene/ferrocene$^+$ (Fc/Fc^+) standard.[51]

Photopatterning. Polymer solution (10 mg/mL P-PN-FLR in toluene) was filtered with a PTFE syringe filter (0.45 μm) and then was spin-casted on ITO glass (800 rpm, 45 s) or silicon wafer (1200 rpm, 45 s). The solution of photoacid generator ((4-phenylthiophenyl)-diphenylsulfonium triflate in methanol, 10 mg/mL) was spin-casted on the top of polymer films with same spin-casting condition in a dark environment. The polymer film was irradiated by the UV flood exposure system (Newport, 1000 W mercury−xenon lamp with midrange UV mirrors: 260−320 nm). The irradiation was conducted through a homemade "UA" stencil (for the patterns in Figure 5a,b and Supporting Information Video S2), or a commercial (SPI Supplies) TEM grid (for the patterns in Figure 5c,d), or a commercial (Photo Etch Technology) stainless steel mask (for the patterns in Supporting Information Figure S8) under the controlled UV intensity (130 mW/cm^2, with calibrator probe of 280 nm, exposure time = 30 s unless the case described below). After UV exposure, the film was soaked in toluene for 5−10 s to remove the nonirradiated polymer and then in methanol for 5−10 s to remove the photoacid residues. The film was rinsed by clean methanol and then was blow-dried by an air gun. The mask for the patterned "UA" letters (Figure 5) was prepared in the lab. In order to get a thick film for the better contrast in the videos, the polymer spin-casting process was repeated for three times with a time interval of 1 min between each spin-

dx.doi.org/10.1021/ma501960t | *Macromolecules* XXXX, XXX, XXX−XXX

coating process to make sure the previous spin-casted film is dry enough. The exposure time for such a film is 2 min.

■ ASSOCIATED CONTENT

Supporting Information

Synthesis details of monomers and polymers, the properties of polymers including NMR spectrum, molecular weight, and TGA information, UV/vis absorption of thermal annealed polymer films before and after solvent washing, electrochromic profile of polymers, optical images of photopatterned P-PN-FLR films, and characterization of the UV irradiated polymers; two videos to demonstrate the electrochromism of patterned polymers. This material is available free of charge via the Internet at http://pubs.acs.org.

■ AUTHOR INFORMATION

Corresponding Author

*E-mail yu.zhu@uakron.edu (Y.Z.).

Notes

The authors declare no competing financial interest.

■ ACKNOWLEDGMENTS

The authors thank E. Laughlin and D. Galehouse for technical support. The authors are grateful for financial support from the University of Akron.

■ REFERENCES

(1) Singh, T. B.; Sariciftci, N. S. *Annu. Rev. Mater. Res.* **2006**, *36*, 199−230.
(2) Forrest, S. R.; Thompson, M. E. *Chem. Rev.* **2007**, *107*, 923−925.
(3) Kim, H. D.; Jeong, J. K.; Chung, H. J.; Mo, Y. G. *SID Symp. Dig. Tech. Pap.* **2008**, *39*, 291−294.
(4) Kim, H. D.; Chung, H.-J.; Berkeley, B. H.; Kim, S. S. *Inf. Disp.* **2009**, *25*, 18−22.
(5) Hirano, T.; Matsuo, K.; Kohinata, K.; Hanawa, K.; Matsumi, T.; Matsuda, E.; Matsuura, R.; Ishibashi, T.; Yoshida, A.; Sasaoka, T. *SID Symp. Dig. Tech. Pap.* **2007**, *38*, 1592−1595.
(6) Lee, S. T.; Suh, M. C.; Kang, T. M.; Kwon, Y. G.; Lee, J. H.; Kim, H. D.; Chung, H. K. *SID Symp. Dig. Tech. Pap.* **2007**, *38*, 1588−1591.
(7) Xu, Y. Y.; Zhang, F.; Feng, X. L. *Small* **2011**, *7*, 1338−1360.
(8) Forrest, S. R. *Nature* **2004**, *428*, 911−918.
(9) Holdcroft, S. *Adv. Mater.* **2001**, *13*, 1753−1765.
(10) Briseno, A. L.; Mannsfeld, S. C. B.; Ling, M. M.; Liu, S. H.; Tseng, R. J.; Reese, C.; Roberts, M. E.; Yang, Y.; Wudl, F.; Bao, Z. N. *Nature* **2006**, *444*, 913−917.
(11) Muller, C. D.; Falcou, A.; Reckefuss, N.; Rojahn, M.; Wiederhirn, V.; Rudati, P.; Frohne, H.; Nuyken, O.; Becker, H.; Meerholz, K. *Nature* **2003**, *421*, 829−833.
(12) Beaujuge, P. M.; Ellinger, S.; Reynolds, J. R. *Nat. Mater.* **2008**, *7*, 795−799.
(13) Amb, C. M.; Dyer, A. L.; Reynolds, J. R. *Chem. Mater.* **2011**, *23*, 397−415.
(14) Menard, E.; Meitl, M. A.; Sun, Y. G.; Park, J. U.; Shir, D. J. L.; Nam, Y. S.; Jeon, S.; Rogers, J. A. *Chem. Rev.* **2007**, *107*, 1117−1160.
(15) Chabinyc, M. L.; Wong, W. S.; Arias, A. C.; Ready, S.; Lujan, R. A.; Daniel, J. H.; Krusor, B.; Apte, R. B.; Salleo, A.; Street, R. A. *Proc. IEEE* **2005**, *93*, 1491−1499.
(16) Sirringhaus, H.; Kawase, T.; Friend, R. H.; Shimoda, T.; Inbasekaran, M.; Wu, W.; Woo, E. P. *Science* **2000**, *290*, 2123−2126.
(17) Yu, J. F.; Holdcroft, S. *Chem. Commun.* **2001**, 1274−1275.
(18) Liu, H. M.; He, J.; Wang, P. F.; Xie, H. Z.; Zhang, X. H.; Lee, C. S.; Sun, B. Q.; Xia, Y. J. *Appl. Phys. Lett.* **2005**, *87*, 221103.
(19) Chou, S. Y.; Krauss, P. R.; Renstrom, P. J. *Science* **1996**, *272*, 85−87.
(20) Yu, J. F.; Holdcroft, S. *Chem. Mater.* **2002**, *14*, 3705−3714.
(21) DeFranco, J. A.; Schmidt, B. S.; Lipson, M.; Malliaras, G. G. *Org. Electron* **2006**, *7*, 22−28.
(22) Taylor, P. C.; Lee, J. K.; Zakhidov, A. A.; Chatzichristidi, M.; Fong, H. H.; DeFranco, J. A.; Malliaras, G. C.; Ober, C. K. *Adv. Mater.* **2009**, *21*, 2314−2317.
(23) Sangermano, M.; Giannelli, S.; Ortiz, R. A.; Duarte, M. L. B.; Gonzalez, A. K. R.; Valdez, A. E. G. *J. Appl. Polym. Sci.* **2009**, *112*, 1780−1787.
(24) Bayerl, M. S.; Braig, T.; Nuyken, O.; Muller, D. C.; Gross, M.; Meerholz, K. *Macromol. Rapid Commun.* **1999**, *20*, 224−228.
(25) Afzali, A.; Dimitrakopoulos, C. D.; Graham, T. O. *Adv. Mater.* **2003**, *15*, 2066−2069.
(26) Bacher, A.; Erdelen, C. H.; Paulus, W.; Ringsdorf, H.; Schmidt, H. W.; Schuhmacher, P. *Macromolecules* **1999**, *32*, 4551−4557.
(27) Crivello, J. V.; Falk, R.; Zonca, M. R. *J. Polym. Sci., Polym. Chem.* **2004**, *42*, 1630−1646.
(28) Xing, K. Z.; Johansson, N. *Adv. Mater.* **1997**, *9*, 1027−1031.
(29) Du, N. Y.; Tian, R. Y.; Peng, J. B.; Mei, Q. B.; Lu, M. G. *Macromol. Rapid Commun.* **2006**, *27*, 412−417.
(30) Scheler, E.; Strohriegl, P. *J. Mater. Chem.* **2009**, *19*, 3207−3212.
(31) Scheler, E.; Strohriegl, P. *Chem. Mater.* **2010**, *22*, 1410−1419.
(32) Solomeshch, O.; Medvedev, V.; Mackie, P. R.; Cupertino, D.; Razin, A.; Tessler, N. *Adv. Funct. Mater.* **2006**, *16*, 2095−2102.
(33) Yang, X. H.; Muller, D. C.; Neher, D.; Meerholz, K. *Adv. Mater.* **2006**, *18*, 948−954.
(34) Kohnen, A.; Riegel, N.; Kremer, J. H. W. M.; Lademann, H.; Muller, D. C.; Meerholz, K. *Adv. Mater.* **2009**, *21*, 879−884.
(35) Lu, K.; Guo, Y. L.; Liu, Y. Q.; Di, C. A.; Li, T.; Wei, Z. M.; Yu, G.; Du, C. Y.; Ye, S. H. *Macromolecules* **2009**, *42*, 3222−3226.
(36) Park, M. J.; Lee, J. I.; Chu, H. Y.; Kim, S. H.; Zyung, T.; Eom, J. H.; Shim, H. K.; Hwang, D. H. *Synth. Met.* **2009**, *159*, 1393−1397.
(37) Charas, A.; Alves, H.; Martinho, J. M. G.; Alcacer, L.; Fenwick, O.; Cacialli, F.; Morgado, J. *Synth. Met.* **2008**, *158*, 643−653.
(38) Rehab, A.; Salahuddin, N. *Polymer* **1999**, *40*, 2197−2207.
(39) Nakayama, Y.; Matsuda, T. *J. Polym. Sci., Polym. Chem.* **1992**, *30*, 2451−2457.
(40) Domercq, B.; Hreha, R. D.; Zhang, Y. D.; Larribeau, N.; Haddock, J. N.; Schultz, C.; Marder, S. R.; Kippelen, B. *Chem. Mater.* **2003**, *15*, 1491−1496.
(41) Reeves, B. D.; Unur, E.; Ananthakrishnan, N.; Reynolds, J. R. *Macromolecules* **2007**, *40*, 5344−5352.
(42) Zambounis, J. S.; Hao, Z.; Iqbal, A. *Nature* **1997**, *388*, 131−132.
(43) Fan, Y.; Zhao, Y.; Ye, L.; Li, B.; Yang, G.; Wang, Y. *Cryst. Growth Des.* **2009**, *9*, 1421−1430.
(44) Smith, P. A. S. *J. Am. Chem. Soc.* **1948**, *70*, 320−323.
(45) Rădulescu, C.; Ioniţă, I.; Hossu, A. M. *Dyes Pigm.* **2005**, *65*, 175−177.
(46) Liu, S.-Y.; Li, H.-Y.; Shi, M.-M.; Jiang, H.; Hu, X.-L.; Li, W.-Q.; Fu, L.; Chen, H.-Z. *Macromolecules* **2012**, *45*, 9004−9009.
(47) Stas, S.; Sergeyev, S.; Geerts, Y. *Tetrahedron* **2010**, *66*, 1837−1845.
(48) Miyaura, N.; Suzuki, A. *Chem. Rev.* **1995**, *95*, 2457−2483.
(49) Ferraro, J. R.; Wu, J. G.; Soloway, R. D.; Li, W. H.; Xu, Y. Z.; Xu, D. F.; Shen, G. R. *Appl. Spectrosc.* **1996**, *50*, 922−927.
(50) Bredas, J. L.; Street, G. B. *Acc. Chem. Res.* **1985**, *18*, 309−315.
(51) Zhu, Y.; Zhang, K.; Tieke, B. *Macromol. Chem. Physic* **2009**, *210*, 431−439.
(52) Dyer, A. L.; Craig, M. R.; Babiarz, J. E.; Kiyak, K.; Reynolds, J. R. *Macromolecules* **2010**, *43*, 4460−4467.
(53) Lundt, B. F.; Johansen, N. L.; Vølund, A.; Markussen, J. *Int. J. Pept. Protein Res.* **1978**, *12*, 258−268.
(54) Ben-Ishai, D.; Berger, A. *J. Org. Chem.* **1952**, *17*, 1564−1570.
(55) Kim, J.; You, J.; Kim, B.; Park, T.; Kim, E. *Adv. Mater.* **2011**, *23*, 4168−4173.